2024 European Control Conference (ECC)
June 25-28, 2024. Stockholm, Sweden

An Efficient Approximation of the Second-Order Extended Kalman Filter for a Class of Nonlinear Systems

Spencer Boone[1] and Jay McMahon[2]

***Abstract*— This paper presents an efficient approximation for the second-order extended Kalman filter (SEKF) for nonlinear systems possessing a dominant direction of nonlinearity, which we call the directional second-order extended Kalman filter (DSEKF). Under certain assumptions, it is shown that the second-order terms in the standard SEKF can be accurately approximated with a single function evaluation (n_x terms). The DSEKF approximation addresses some of the drawbacks of the standard SEKF - namely, that the SEKF requires deriving the second-order state rates for the system, and requires integrating an additional n_x^3 terms on top of the first-order extended Kalman filter (EKF). The resulting algorithm is an efficient alternative to sampling-based nonlinear filtering methods. The DSEKF can also be easily added onto existing operational systems that already use the EKF.**

I. Introduction

Nonlinear filtering methods are required to estimate states for vehicles operating in nonlinear systems where linearized filtering methods such as the extended Kalman filter (EKF) are insufficiently accurate. Such methods include sampling-based methods, such as the unscented Kalman filter (UKF) [1] or the particle filter [2], or methods based on second or higher-order Taylor series expansions of the dynamics around a reference [3], such as the second-order extended Kalman filter (SEKF) [4]. The SEKF suffers from several drawbacks that have limited its use in operational applications. Namely, the SEKF requires integrating an additional n_x^3 terms to perform the filter time update (where n_x is the state vector size) in addition to the integration requirements of the first-order EKF (which will generally be $n_x^2 + n_x$). For real-life dynamic systems, analytic formulations for the second-order derivatives of the dynamics are not always available, in which case the SEKF also requires deriving the second-order state rates in order to numerically compute these derivatives. This can be a costly or infeasible process.

As a result of these drawbacks, the unscented Kalman filter has emerged as a more popular form of nonlinear filter. The UKF time update relies on integrating a number of sigma points through the nonlinear dynamics, and approximating the resulting state statistics using the distribution of these points. The UKF does not require deriving the state rates of the dynamics. However, the UKF does require tuning several parameters to control the spread of the sigma point samples, which in practice can be a cumbersome process. Several numerical approximations for the SEKF have been developed using either sigma points [5] or central differencing [6] to approximate the higher-order derivatives or moments of the dynamics. Inspired by these methods, we propose a further approximation strategy suitable for nonlinear systems that possess a dominant direction of nonlinearity.

For a number of applications, in particular in the field of spacecraft navigation, the current operational algorithms use the first-order extended Kalman filter [7]. These algorithms may be implemented in complex software systems with legacy components that are difficult to modify. Applying these tools to more complex and nonlinear dynamic systems will require nonlinear filtering methods; however, implementing an entirely new type of filter such as the sampling-based UKF is not always desirable. This provides the catalyst for this work, which is to derive an efficient approximation of the SEKF that has minimal tuning parameters, and can be easily added onto an existing implementation of the first-order EKF. This work is motivated by deep-space spacecraft navigation applications, where the dynamics are highly nonlinear, and significant measurement gaps are frequently encountered, which allow nonlinear effects to become relatively important in the propagation of state uncertainties [8].

For many nonlinear systems, there will be a dominant direction along which the second-order terms will be significantly larger than all other second-order terms. For this class of systems, the second-order effects can be approximated using only these most important second-order terms, and ignoring all other terms. This property has been numerically demonstrated by the authors of this work for efficient nonlinear spacecraft uncertainty propagation and navigation applications [9], [10].

In this work we formally derive the approximate SEKF using this property, yielding what we call the directional second-order extended Kalman filter (DSEKF). We then introduce an approximation for the second-order directional derivative of the dynamics which only requires a single function evalution (i.e., state integration) in addition to the standard EKF requirements. The resulting algorithm can accurately approximate the full SEKF for the class of nonlinear systems with a single dominant direction of nonlinearity. Since it requires only integrating n_x terms in addition to the first-order EKF, the scaling of the resulting algorithm as n_x increases is comparable to that of the first-order EKF. It is also a straightforward extension to include in any existing operational implementation of the EKF.

This paper is organized as follows. First, we introduce the dynamics model, second-order expansion of the dynamics, and the second-order state mean and covariance propagation

[1]Spencer Boone is currently affiliated with ISAE SUPAERO, Toulouse, France spencer.boone@isae-supaero.fr

[2] Jay McMahon is affiliated with the Smead Department of Aerospace Engineering Sciences, University of Colorado Boulder, Boulder, CO, USA jay.mcmahon@colorado.edu

equations. Next, we derive the approximation for the second-order dynamics expansion, provide the resulting simplified uncertainty propagation equations, and propose a further numerical approximation strategy. Using these equations, we then derive the directional second-order extended Kalman filter. We apply the DSEKF to an example of a spacecraft operating in cislunar space, a nonlinear dynamic system subject to significant gaps between measurement passes.

II. Preliminary

A. Notation

In this work, vectors are shown in boldface. Index notation is used to represent multi-dimensional tensors. Superscripts indicate components of a vector, matrix, or tensor. The order of a tensor is determined by the number of superscript indices. Subscripts indicate the time of a vector, or for a matrix or tensor, (t_{k+1}, t_k) indicates a mapping from t_k to t_{k+1}.

B. Model

Consider a time-varying nonlinear dynamic system. Let $\boldsymbol{x}_k \in \mathbb{R}^{n_x}$ be the state vector at time $t_k, k = 0, 1, ..., N-1$. The system can be expressed as:

$$\boldsymbol{x}_{k+1} = f(\boldsymbol{x}_k, t_{k+1}) \tag{1}$$

where f represents the nonlinear solution flow of the system, i.e. the nonlinear mapping of the state from time t_k to t_{k+1}.

C. Taylor Series Expansion

The deviation of the current state $\boldsymbol{x}_{k+1}$ from a reference trajectory $\hat{\boldsymbol{x}}_{k+1}$ can be represented using the solution flow notation:

$$\delta\boldsymbol{x}_{k+1} = f(\hat{\boldsymbol{x}}_k + \delta\boldsymbol{x}_k, t_{k+1}) - f(\hat{\boldsymbol{x}}_k, t_{k+1}) \tag{2}$$

For a standard or extended Kalman filter formulation, this deviation is approximated by performing a Taylor series expansion around the reference trajectory $\hat{\boldsymbol{x}}_k$ and truncating to first order (i.e., linearizing around $\hat{\boldsymbol{x}}_k$), giving

$$\delta x^i_{k+1} \simeq \phi^{i,\kappa_1}_{(t_{k+1},t_k)} \delta x^{\kappa_1}_k + H.O.T. \tag{3}$$

where the first-order coefficient $\phi^{i,\kappa_1}_{(t_{k+1},t_k)} \in \mathbb{R}^{n_x \times n_x}$ in this expansion is the well-known state transition matrix (STM). It is possible to include higher-order terms in this expansion, yielding what are known as the state transition tensors (STTs).

Definition 1 (State transition tensor): The second-order state transition tensor (STT) $\phi^{i,\kappa_1\kappa_2}_{(t_{k+1},t_k)} \in \mathbb{R}^{n_x \times n_x \times n_x}$ is the second-order term in the Taylor series expansion of a dynamic system around a reference $\hat{\boldsymbol{x}}_k$. It is defined as

$$\phi^{i,\kappa_1\kappa_2}_{(t_{k+1},t_k)} = \left.\frac{\partial^2(x^i_{k+1})}{\partial x^{\kappa_1}_k \partial x^{\kappa_2}_k}\right|_{\boldsymbol{x}_k = \hat{\boldsymbol{x}}_k} \tag{4}$$

Including the second-order STT in the Taylor series expansion in Eq. 3 second-order terms yields

$$\delta x^i_{k+1} \simeq \phi^{i,\kappa_1}_{(t_{k+1},t_k)} \delta x^{\kappa_1}_k + \frac{1}{2}\phi^{i,\kappa_1\kappa_2}_{(t_{k+1},t_k)} \delta x^{\kappa_1}_k \delta x^{\kappa_2}_k \tag{5}$$

For most applications, this STT must be numerically integrated along with the state vector, which can constitute a significant computational burden. The differential equations to integrate the STM and second-order STT are:

$$\dot{\phi}^{i,a} = A^{i,\alpha}\phi^{\alpha,a} \tag{6}$$

$$\dot{\phi}^{i,ab} = A^{i,\alpha}\phi^{\alpha,ab} + A^{i,\alpha\beta}\phi^{\alpha,a}\phi^{\beta,b} \tag{7}$$

where the A matrix and tensor represent the first and second-order partial derivatives of the state rates with respect to the state, and the timespans are omitted for conciseness.

D. Nonlinear uncertainty propagation

Next, consider the state vector to be a Gaussian random vector $\boldsymbol{x}_k \sim \mathcal{N}(\boldsymbol{m}_k, P_k)$, where $\boldsymbol{m}_k$ is the mean state vector and P_k is the covariance matrix at time t_k. The STM can be used to perform a linear propagation of a vehicle's mean state and covariance through the linearized dynamics (omitting the timespan for conciseness):

$$\delta m^i_{k+1} = \phi^{i,\kappa_1}\delta m^{\kappa_1}_k \tag{8}$$

$$P^{ij}_{k+1} = \phi^{i,\kappa_1}\phi^{j,\eta_1}P^{i,\kappa_1\eta_1}_k - \delta m^i_{k+1}\delta m^j_{k+1} \tag{9}$$

In the EKF formulation, the Taylor series expansion is performed around the current best estimate of the mean state, giving $\delta\boldsymbol{m}_k = 0$, which reduces Eqs. 8 and 9 to:

$$\delta m^i_{k+1} = 0 \tag{10}$$

$$P^{ij}_{k+1} = \phi^{i,\kappa_1}\phi^{j,\eta_1}P^{i,\kappa_1\eta_1}_k \tag{11}$$

The second-order STT can be used to analytically propagate a vehicle state's mean and covariance through nonlinear dynamics, following Ref. [11]. For the case where $\delta\boldsymbol{m}_k = 0$, these equations are

$$\delta m^i_{k+1} = \frac{1}{2}\phi^{i,\kappa_1\kappa_2}P^{\kappa_1\kappa_2}_k \tag{12}$$

$$P^{ij}_{k+1} = \phi^{i,\kappa_1}\phi^{j,\eta_1}P^{i,\kappa_1\eta_1}_k + \frac{1}{4}\phi^{i,\kappa_1\kappa_2}\phi^{j,\eta_1\eta_2} \times \left[P^{\kappa_1\eta_1}_k P^{\kappa_2\eta_2}_k + P^{\kappa_1\eta_2}_k P^{\kappa_2\eta_1}_k\right] \tag{13}$$

One can recognize that setting all the second-order STT terms ($\phi^{i,\kappa_1\kappa_2}$) to zero returns the linear covariance propagation equations.

III. Approximating Second-Order Dynamics

A. Motivation

For a n_x-dimensional state vector, the second-order STT is a tensor of dimension $n_x \times n_x \times n_x$, and thus has n_x^3 elements. Numerically integrating this STT represents a significant computational burden on top of the first-order STM integration, which has n_x^2 elements. For example, for $n_x = 6$, the STM will have 36 elements, while the second-order STT will have 216. It is therefore beneficial to derive an approximation for this STT that includes only the most important elements.

B. Directional state transition tensor

The second-order term in Eq. 5 can also be thought of as a summation of n_x^2 vector terms:

$$\delta \boldsymbol{x}_{k+1,\kappa_1\kappa_2} = \sum_{i=1}^{n_x} \frac{1}{2}\phi^{i,\kappa_1\kappa_2}\delta x_k^{\kappa_1}\delta x_k^{\kappa_2} \tag{14}$$

for fixed $\kappa_1 \in [1, n_x]$ and $\kappa_2 \in [1, n_x]$. In Ref. [9], the authors of this work showed that if one of these terms is significantly larger than all other terms, for example,

$$\mathcal{O}\left(\|\delta \boldsymbol{x}_{k+1,11}\|\right) \gg \mathcal{O}\left(\|\delta \boldsymbol{x}_{k+1,1\ldots n_x,2\ldots n_x}\|\right) \tag{15}$$

then the full second-order effects from Eq. 5 can be approximated as

$$\frac{1}{2}\phi^{i,\kappa_1\kappa_2}\delta x_k^{\kappa_1}\delta x_k^{\kappa_2} \simeq \frac{1}{2}\phi^{i,11}\delta x_k^1\delta x_k^1 \tag{16}$$

where $\phi^{i,11}$ is a vector of size n_x containing the STT derivatives only with respect to the first state component. By using this approximation, the number of elements required to model the second-order effects is reduced from n_x^3 to n_x, which represents a significant reduction in storage and computational requirements.

It is unlikely that using a standard Cartesian state representation will result in the STT term along a particular direction dominating over other terms, as required in Eq. 15. We can, however, take the derivatives of the STT with respect to a rotated orthogonal basis $\boldsymbol{y} \in \mathbb{R}^{n_y}$ that is formed through a linear combination of the state coordinates. For $n_y = n_x$, the rotated STT will exactly match the standard second-order STT. For $n_y < n_x$, the rotated STT becomes an approximation of the full STT, with $\phi^{i,\gamma_1\gamma_2} \in \mathbb{R}^{n_x \times n_y \times n_y}$.

For many applications, in particular in the field of spacecraft dynamics, the nonlinear dynamics possess a single direction along which the nonlinear terms dominate over all other directions. For these applications, we can reduce the rotated STT basis size to $n_y = 1$, giving what we call the *directional* state transition tensor (DSTT).

Definition 2 (Directional state transition tensor): The second-order directional state transition tensor (DSTT) $\boldsymbol{\psi}_{[2]} \in \mathbb{R}^{n_x}$ is defined as

$$\psi_{[2]}^i = \left.\frac{\partial^2(x_{k+1}^i)}{\partial y_k \partial y_k}\right|_{y_k = \boldsymbol{R}\hat{\boldsymbol{x}}_k} \tag{17}$$

where $\boldsymbol{R} \in \mathbb{R}^{n_x}$ is the transformation vector mapping the standard Cartesian basis to the DSTT direction.

The DSTT represents a significant reduction in the number of elements when compared to the full STT. For example, for $n_x = 6$, the number of second-order elements is reduced from 216 down to just 6. In this work we consider the case where the full first-order STM is computed with respect to the standard Cartesian basis $\boldsymbol{x} \in \mathbb{R}^{n_x}$, and the second-order DSTT is computed with respect to the single direction $y \in \mathbb{R}^1$. Letting $\delta y_k = \boldsymbol{R}\delta \boldsymbol{x}_k$, then Eq. 5 can be approximated with the second-order DSTT as (recognizing that δy_k is a scalar):

$$\delta x_{k+1}^i \simeq \phi^{i,\kappa_1}\delta x_k^{\kappa_1} + \psi_{[2]}^i \delta y_k \delta y_k \tag{18}$$

$\boldsymbol{\psi}_{[2]}$ can be numerically integrated along with the STM using the following equations:

$$\dot{\phi}^{i,a} = A^{i,\alpha}\phi^{\alpha,a} \tag{19}$$

$$\dot{\psi}_{[2]}^i = A^{i,\alpha}\psi_{[2]}^\alpha + A^{i,\alpha\beta}\phi^{\alpha,a}\phi^{\beta,b}R^aR^b \tag{20}$$

Note the presence of the second-order state rate tensor $A^{i,\alpha\beta}$ in Eq. 20. While existing systems will likely have already implemented analytic or numerical methods to compute the first-order state rate matrix $A^{i,\alpha}$ in order to obtain the STM, it is not always simple or desired to extend these methods to compute $A^{i,\alpha\beta}$. In Section III-E, we propose a simple numerical approximation strategy to avoid computing this term using a single function evaluation.

C. Approximate nonlinear uncertainty propagation

If we are using Eq. 18 to approximate the second-order effects, then we can greatly simplify the nonlinear mean and covariance propagation equations from Eqs. 12 and 13. First, we can simplify higher-order calculations involving the covariance matrix through the following transformation

$$\sigma_{k,R} = \sqrt{R^i P_k^{ij} R^j} \tag{21}$$

$\sigma_{k,R}$ is a scalar that refers to the 1-σ uncertainty along the DSTT direction. Eqs. 12 and 13 thus reduce to

$$\delta m_{k+1}^i = \frac{1}{2}\psi_{[2]}^i \sigma_{k,R}^2 \tag{22}$$

$$P_{k+1}^{ij} = \phi^{i,\kappa_1}\phi^{j,\eta_1}P_k^{\kappa_1\eta_1} + \frac{1}{2}\sigma_{k,R}^2\psi_{[2]}^i\psi_{[2]}^j \tag{23}$$

Besides the computational savings in obtaining or integrating $\boldsymbol{\psi}_{[2]}$ instead of $\phi^{i,\kappa_1\kappa_2}$, the computations involving these terms are far simpler in Eqs. 22 and 23 than in Eqs. 12 and 13.

D. Direction selection

There is not always an intuitive direction along which to compute the DSTT derivatives. Recall that the objective is to find a direction along which Eq. 15 holds. For some systems, physical intuition into the dynamics may be sufficient to determine the best direction. For example, for a spacecraft operating in two-body dynamics, it is a well-known property that for long integration times, any deviation in the in-track velocity direction will result in the largest deviations.

For most systems, there is no such obvious direction. It is therefore beneficial to use insights provided by the STM and/or STT to identify the dominant direction of nonlinearity. Since the objective is this work is to avoid computing the full STT, we will rely on the STM to compute this direction, using the Cauchy-Green Tensor (CGT) [12], [9]

Definition 3 (Cauchy-Green tensor): The CGT is defined as

$$C = \phi_{(t_{k+1},t_k)}^T \phi_{(t_{k+1},t_k)} \tag{24}$$

The eigenvalues λ_{ξ_γ} and eigenvectors $\boldsymbol{\xi}_\gamma$ of the CGT have the relation $\|\phi_{(t_{k+1},t_k)}\boldsymbol{\xi}_\gamma\| = \sqrt{\lambda_{\xi_\gamma}}\|\boldsymbol{\xi}_\gamma\|$. Thus, if $\lambda_{max} \gg \lambda_{other}$, then

$$\|\delta \boldsymbol{x}_{k+1,max}^{[1]}\| \gg \|\delta \boldsymbol{x}_{k+1,other}^{[1]}\| \tag{25}$$

where $\delta \boldsymbol{x}^{[1]}_{k+1,max}$ refers to the first-order term in the Taylor series expansion along the direction corresponding to the maximum eigenvalue, and $\delta \boldsymbol{x}^{[1]}_{k+1,other}$ refers to the first-order terms along all other directions.

The CGT only provides exact information about the maximum *linear* stretching direction. However, for the class of nonlinear systems with a dominant stretching direction, we assume that the maximum linear stretching direction obtained from an eigendecomposition of the Cauchy-Green Tensor generally aligns with the maximum second-order stretching direction if $\lambda_{max} \gg \lambda_{other}$. This property has been numerically validated by the authors of this work in Refs. [9] and [10].

In order to demonstrate why this assumption holds for this class of nonlinear system, consider that the multivariate Taylor series expansion in Eq. 5 can be thought of as a summation of multiple convergent series along each state component or direction. From Eq. 25:

$$\lambda_{max} \gg \lambda_{other} \implies \|\delta \boldsymbol{x}^{[1]}_{k+1,max}\| \gg \|\delta \boldsymbol{x}^{[1]}_{k+1,other}\| \tag{26}$$

If we assume the Taylor series expansion is convergent within its region of validity, this implies that

$$\|\delta \boldsymbol{x}^{[2]}_{k+1,max}\| < \|\delta \boldsymbol{x}^{[1]}_{k+1,max}\| \tag{27}$$

$$\|\delta \boldsymbol{x}^{[2]}_{k+1,other}\| < \|\delta \boldsymbol{x}^{[1]}_{k+1,other}\| \tag{28}$$

Combining Eqs. 26-28, the bound on the second-order term along the maximum linear stretching direction will be significantly larger than the bound on all other second-order terms. This implies that the maximum second-order stretching direction will generally align with this direction. As λ_{max} becomes more dominant over λ_{other}, these bounds become more disparate.

For the remainder of this work, we will assume that the DSTT direction $\boldsymbol{R}$ is the linear maximum stretching direction obtained from the CGT eigendecomposition.

E. Efficient Numerical Approximation

Integrating the second-order DSTT in Eq. 20 can represent a significant burden on top of integrating the first-order STM (Eq. 19), since the second-order state rate tensor $A^{i,\alpha\beta}$ must be computed at each integration step. We therefore propose the following approximation for the second-order DSTT.

Proposition 1: Assuming the STM has been obtained (analytically or numerically), the second-order DSTT $\boldsymbol{\psi}_{[2]}$ can be approximated with a single state integration perturbed from the reference state along the DSTT direction $\boldsymbol{R}$.

Proof: Inserting Eq.18 into Eq. 2 and letting $\delta \boldsymbol{x}_k = \varepsilon \boldsymbol{R}$, where $\varepsilon \ll 1$, we obtain

$$\phi^{i,\kappa_1}\varepsilon R^{\kappa_1} + \frac{1}{2}\psi^i_{[2]}\varepsilon^2 \approx f(\hat{\boldsymbol{x}}_{k+1} + \varepsilon \boldsymbol{R}, t_{k+1}) - f(\hat{\boldsymbol{x}}_k, t_{k+1}) \tag{29}$$

Isolating for $\boldsymbol{\psi}_{[2]}$ gives:

$$\psi^i_{[2]} \approx \frac{2\left[f(\hat{\boldsymbol{x}}_k + \varepsilon \boldsymbol{R}, t_{k+1}) - f(\hat{\boldsymbol{x}}_k, t_{k+1}) - \phi^{i,\kappa_1}\varepsilon R^{\kappa_1}\right]}{\varepsilon^2} \tag{30}$$

Since the other terms are required for the first-order EKF, only the additional single function evaluation $f(\hat{\boldsymbol{x}}_k + \varepsilon R, t_k)$ is required to approximate the full second-order effects. ■

By using this approximation, we obviate the need to computing the second-order state rate tensor $A^{i,\alpha\beta}$. The size of the parameter ε can be viewed as a tuning parameter that has now been introduced into the algorithm.

IV. Second-Order Extended Kalman Filter

We will now develop the directional second-order extended Kalman filter (DSEKF) using the approximations derived in Section III. A Kalman filter consists of two steps: a time update and a measurement update. We use $\boldsymbol{m}^-_{k+1}$ and P^-_{k+1} to refer to the state estimate and associated covariance matrix prior to the measurement update, and $\boldsymbol{m}^+_{k+1}$ and P^+_{k+1} to refer to the state estimate and covariance matrix after the measurement update.

In this work, we only consider the second-order terms in the time update. The measurement update can similarly be expanded to include second or higher-order terms (e.g., see Ref. [3]); this will be the focus of future work. For conciseness, we also do not include the effects of process noise in the dynamics model, though this is a straightforward addition.

A. Time Update

The time update for a Kalman filter propagates a mean state $\boldsymbol{m}_k$ with covariance P_k from time t_k to time t_{k+1}. Under the extended Kalman filter formulation, the reference trajectory is reinitialized at the state estimate after each update (giving $\mathbb{E}[\delta \mathbf{x}^+_k] = \delta \boldsymbol{m}^+_k = 0$).

1) EKF: The first-order time update is

$$(m^-_{k+1})^i = f^i(\boldsymbol{m}^+_k, t_{k+1}) \tag{31}$$

$$(P^-_{k+1})^{ij} = \phi^{i,\kappa_1}\phi^{j,\kappa_2}(P^+_k)^{\kappa_1\kappa_2} + Q_k \tag{32}$$

where Q_k is the process noise covariance matrix.

2) SEKF: Eqs. 12 and 13 can be used to formulate the second-order Kalman filter time update, which can better capture nonlinear dynamics.

$$(m^-_{k+1})^i = f^i(\boldsymbol{m}^+_k, t_{k+1}) + \frac{1}{2}\phi^{i,\kappa_1\kappa_2}(P^+_k)^{\kappa_1\kappa_2} \tag{33}$$

$$(P^-_{k+1})^{ij} = \phi^{i,\kappa_1}\phi^{j,\kappa_2}(P^+_k)^{\kappa_1\kappa_2} + \frac{1}{4}\phi^{i,\kappa_1\kappa_2}\phi^{j,\kappa_3\kappa_4}\times \left[(P^+_k)^{\kappa_1\kappa_3}(P^+_k)^{\kappa_2\kappa_4} + (P^+_k)^{\kappa_1\kappa_4}(P^+_k)^{\kappa_2\kappa_3}\right] + Q_k \tag{34}$$

3) DSEKF: Using the second-order DSTT approximation along a single direction, and using the notation from Eqs. 17 and 21, the second-order time update equations reduce to

$$(m^-_{k+1})^i = f^i(\boldsymbol{m}^+_k, t_{k+1}) + \frac{1}{2}\psi^i_{[2]}\sigma^2_{\boldsymbol{R}} \tag{35}$$

$$(P^-_{k+1})^{ij} = \phi^{i,\kappa_1}\phi^{j,\kappa_2}(P^+_k)^{\kappa_1\kappa_2} + \frac{1}{2}\psi^i_{[2]}\psi^j_{[2]}\sigma^2_{\boldsymbol{R}} + Q_k \tag{36}$$

Algorithm 1 provides an example of how to efficiently perform this time update using the numerical approximation method from Sec. III-E.

Algorithm 1 DSEKF time update with numerical approximation

1: **Given:** Mean state estimate $\boldsymbol{m}_k^+$ with associated covariance P_k^+
2: Integrate mean state $\boldsymbol{m}_k^+$ and STM to time t_{k+1} to obtain $f(\boldsymbol{m}_k^+, t_{k+1})$ and $\phi^{i,\kappa_1}_{(t_{k+1},t_k)}$ using Eqs. 1 and 7.
3: Compute the CGT C using Eq. 24
4: Set $\boldsymbol{R} = \boldsymbol{\xi}_{\lambda_{max}}$, the direction associated with the maximum eigenvalue of C
5: Evaluate $f(\boldsymbol{m}_k^+ + \varepsilon \boldsymbol{R}, t_{k+1})$
6: Compute $\boldsymbol{\psi}_{[2]}$ using Eq. 30
7: Compute $\boldsymbol{m}_{k+1}$ and P_{k+1} using Eqs. 35 and 36

We note that this approximation can be considered a simplification of the second-order central differences Kalman filter developed in Ref. [6].

B. Measurement update

The linearized measurement update equations are:

$$\begin{aligned}\left(n_{k+1}^-\right)^i &= h^i\left(\boldsymbol{m}_{k+1}^-, t_{k+1}\right)\\ \left(P_{k+1}^{zz}\right)^- &= \left(H_{k+1}P_{k+1}^- H_{k+1}^T + R_{k+1}\right)\\ \left(P_{k+1}^{xz}\right)^- &= \left(P_{k+1}^- H_{k+1}^T\right)\end{aligned}$$

The optimal measurement update is then provided by,

$$\begin{aligned}K_{k+1} &= P_{k+1}^{xz}\left(P_{k+1}^{zz}\right)^{-1}\\ \boldsymbol{m}_{k+1}^+ &= \boldsymbol{m}_{k+1}^- + K_{k+1}\left(\boldsymbol{z}_{k+1} - \boldsymbol{n}_{k+1}^-\right)\\ P_{k+1}^+ &= P_{k+1}^- - K_{k+1}P_{k+1}^{zz}K_{k+1}^T\end{aligned}$$

where K_k is the Kalman gain matrix at time t_k, P_k^{xz} is the cross-covariance matrix of the state, P_k^{zz} is the covariance matrix of the measurement residual, $\boldsymbol{z}_k$ is the measurement, $\boldsymbol{h}(\boldsymbol{m}_k^-, t_k)$ is the measurement function, H_k is the measurement partial, $\boldsymbol{n}_k^-(\boldsymbol{m}_k^-, t_k)$ is the prefit expectation of the measurement, and R_k is the measurement noise covariance matrix associated with the particular measurement technique.

V. Numerical Example

We will demonstrate the usefulness of the DSEKF on a navigation problem for a spacecraft operating in cislunar space.

A. Dynamics Model

The dynamics of the Earth-Moon system can be approximated using the circular restricted three-body problem (CR3BP). The equations of motion for the CR3BP are

$$\ddot{x} = 2\dot{y} + x - \frac{(1-\mu)(x+\mu)}{r_1^3} - \frac{\mu(-1+x+\mu)}{r_2^3} \tag{37}$$

$$\ddot{y} = -2\dot{x} + y - \frac{y(1-\mu)}{r_1^3} - \frac{\mu y}{r_2^3} \tag{38}$$

$$\ddot{z} = -\frac{z(1-\mu)}{r_1^3} - \frac{\mu z}{r_2^3} \tag{39}$$

where the state vector contains three position (x, y, z) and three velocity $(\dot{x}, \dot{y}, \dot{z})$ terms. In the CR3BP, μ is the ratio of the mass of the secondary body to the total system mass. The system dynamics are modeled in a rotating frame. The distances r_1 and r_2 are defined as the distances from the spacecraft to the primary and secondary bodies, respectively.

B. Scenario Setup

We consider a spacecraft operating in a near rectilinear halo orbit (NRHO) in the vicinity of the Moon. NRHOs are of interest to the wider space community, as they are the planned location for NASA's next manned human space station, the Lunar Gateway [13]. The NRHO is a relatively stable periodic orbit that is characterized by a highly nonlinear perilune region [8], which has led to challenges for standard linearized orbit determination algorithms such as the EKF [14]. These previous studies have found that tracking cadences with long measurement gaps and including measurement passes during the sensitive perilune region can result in filter divergence after several revolutions.

For the measurement model, we approximate realistic passes of the Deep Space Network. We consider two 8-hour passes (one at apolune and one at perilune) with range and range-rate measurements taken every 60 seconds, taken with respect to the system origin. The NRHO and measurement cadence are shown in Fig. 1. The initial NRHO state, initial covariance values, and measurement noise values are given in Table I. We assume no process noise ($Q_k = \mathbf{0}$) for this simplified scenario.

C. Results

Four different Kalman filter setups were simulated for 10 periods of the NRHO: the EKF, the SEKF, the UKF, and the DSEKF (using the numerical approximation, see Algorithm 1). For the nonlinear filters, the nonlinear time update is only used between the long measurement gaps; during the DSN passes, the EKF time update is used due to the short timespans between measurements. 25 iterations of the filters were run for each tracking cadence. An initial estimate error was added to the initial state estimate for each iteration, sampled from a zero-mean distribution with the 1σ values from Table I.

RMS error estimate values for the four different filters are shown in Fig. 2. The EKF does not perform well for this scenario, while the three nonlinear filters perform comparably. In particular, the DSEKF approaches the performance of the

TABLE I: Earth-Moon NRHO scenario parameters

Parameter	Value
μ	0.0121505856
x_0	1.013417655693384
y_0	0.0
z_0	-0.175374764978708
$\dot{x}_0$	0.0
$\dot{y}_0$	-0.083721347178432
$\dot{z}_0$	0.0
1σ pos. uncert.	10 km
1σ vel. uncert.	10 cm/s
Range meas. noise	1 m
Range rate meas. noise	1 mm/s
ε	1e-5

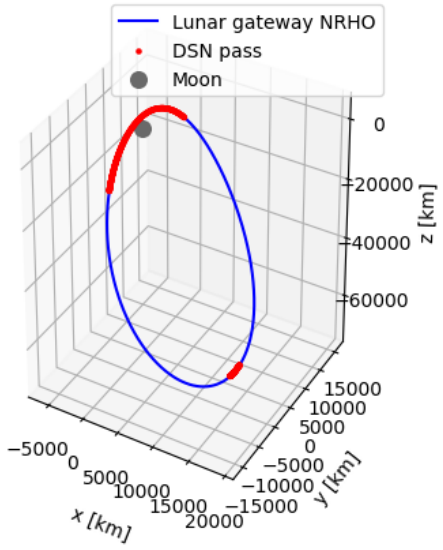

Fig. 1: Spacecraft in NRHO with one 8-hour apolune pass and one 8-hour perilune pass

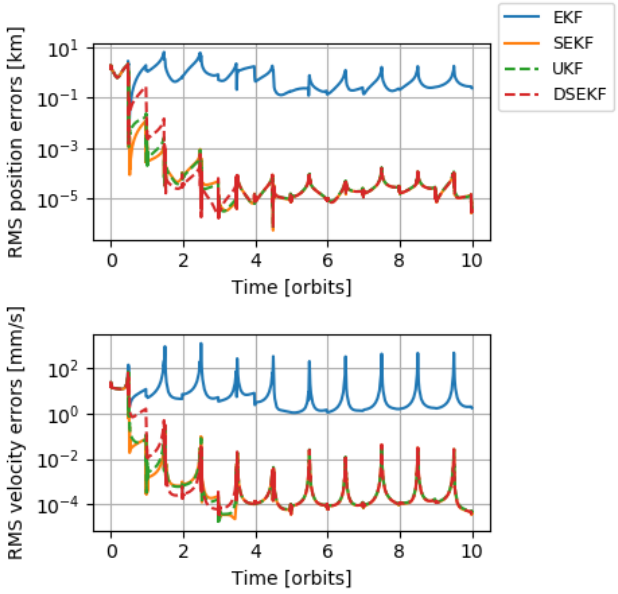

Fig. 2: RMS errors for NRHO scenario using various filters

full SEKF, while only requiring a single additional function evaluation. The average total time to compute the nonlinear time updates for each filter is shown in Table II, along with the final position and velocity RMS error values. The DSEKF is the most efficient of the nonlinear filters, requiring only 25% more computation time than the EKF, while the SEKF and UKF both require over 150% more.

VI. Conclusions

In this work we present the directional second-order extended Kalman filter (DSEKF), an efficient approximation for the second-order extended Kalman filter that is applicable to nonlinear systems that possess a dominant direction of nonlinearity. For this class of systems, the second-order effects can be accurately approximated using only a single function evaluation (i.e., integrating a single state), reducing the number of second-order elements to integrate from n_x^3 to n_x. The advantages of this algorithm over other popular nonlinear filtering methods such as the unscented Kalman filter are that it has fewer parameters that require tuning, and can easily be added onto existing systems that already use the first-order extended Kalman filter. Future work will involve deriving a nonlinear directional measurement update, and evaluating the applicability of the filter to other nonlinear dynamic systems.

TABLE II: Filter performance metrics for NRHO scenario

Filter	Time [s]	Final position RMS error estimate [m]	Final velocity RMS error estimate [mm/s]
EKF	1.73	2.38×10^{-1}	1.75
SEKF	4.67	3.11×10^{-6}	3.90×10^{-5}
UKF	4.68	4.42×10^{-6}	4.89×10^{-5}
DSEKF	2.18	3.20×10^{-6}	3.90×10^{-5}

References

[1] S. J. Julier, J. K. Uhlmann, and H. F. Durrant-Whyte, "A new approach for filtering nonlinear systems," in *Proceedings of 1995 American Control Conference-ACC'95*, vol. 3. IEEE, 1995, pp. 1628–1632.

[2] N. J. Gordon, D. J. Salmond, and A. F. Smith, "Novel approach to nonlinear/non-gaussian bayesian state estimation," in *IEE proceedings F (radar and signal processing)*, vol. 140, no. 2. IET, 1993, pp. 107–113.

[3] R. S. Park and D. J. Scheeres, "Nonlinear semi-analytic methods for trajectory estimation," *Journal of Guidance, Control, and Dynamics*, vol. 30, no. 6, pp. 1668–1676, 2007.

[4] M. Athans, R. Wishner, and A. Bertolini, "Suboptimal state estimation for continuous-time nonlinear systems from discrete noisy measurements," *IEEE Transactions on Automatic Control*, vol. 13, no. 5, pp. 504–514, 1968.

[5] M. Roth and F. Gustafsson, "An efficient implementation of the second order extended kalman filter," in *14th International Conference on Information Fusion*, 2011, pp. 1–6.

[6] K. Ito and K. Xiong, "Gaussian filters for nonlinear filtering problems," *IEEE Transactions on Automatic Control*, vol. 45, no. 5, pp. 910–927, 2000.

[7] J. Sullivan and C. D'Souza, "Extended kalman filter performance on the artemis-1 mission," in *2023 AAS Guidance, Navigation and Control Conference*, 2023.

[8] E. Jenson and D. Scheeres, "Semianalytical measures of nonlinearity based on tensor eigenpairs," in *2021 AAS/AIAA Astrodynamics Specialist Conference*, 2021.

[9] S. Boone and J. McMahon, "Directional state transition tensors for capturing dominant nonlinear effects in orbital dynamics," *Journal of Guidance, Control, and Dynamics*, vol. 46, no. 3, pp. 1–12, 0.

[10] S. Boone, O. Boodram, and J. McMahon, "Efficient nonlinear filtering techniques for near rectilinear halo orbit navigation," in *2023 AAS Guidance, Navigation and Control Conference*, 2023.

[11] R. Park and D. Scheeres, "Nonlinear mapping of gaussian statistics: Theory and applications to spacecraft trajectory design," *Journal of Guidance, Control, and Dynamics*, vol. 29, 2006.

[12] C. Short, K. Howell, A. Haapala, and D. Dichmann, "Mode analysis for long-term behavior in a resonant earth-moon trajectory," *Journal of the Astronautical Sciences*, vol. 64, pp. 156–187, 2017.

[13] E. Zimovan, K. Howell, and D. Davis, "Near rectilinear halo orbits and their application in cis-lunar space," in *3rd IAA Conference on Dynamics and Controls of Space Systems*, 2017.

[14] M. J. Bolliger, M. Thompson, N. Re, C. Ott, and D. Davis, "Ground-based navigation trades for operations in gateway's near rectilinear halo orbit," in *31st AAS/AIAA Space Flight Mechanics Meeting*, 2021.